Sādhanā Vol. 41, No. 10, October 2016, pp. 1219–1234
DOI 10.1007/s12046-016-0546-z

Machinability evaluation of Al–4%Cu–7.5%SiC metal matrix composite by Taguchi–Grey relational analysis and NSGA-II

V SELVAKUMAR[1], S MURUGANANDAM[2], T TAMIZHARASAN[3] and N SENTHILKUMAR[4,*]

[1]Mahalakshmi Engineering College, Tiruchirapalli, Tamil Nadu 621213, India
[2]K. Ramakrishnan College of Technology, Tiruchirappalli, Tamil Nadu 621112, India
[3]Periyar Maniammai University, Thanjavur, Tamil Nadu 613403, India
[4]Adhiparasakthi Engineering College, Melmaruvathur, Tamil Nadu 603319, India
e-mail: nsk@adhiparasakthi.in

MS received 26 December 2015; accepted 14 May 2016

Abstract. Machinability evaluation of Al–4%Cu–7.5%SiC metal matrix composite (MMC) prepared by powder metallurgy (P/M) process is presented. Specimens are prepared with 99.85% pure aluminum added with 4% copper and 7.5% silicon carbide particles by volume fraction. Scanning electron microscope image shows even distribution of particles in Al-MMC. Turning operation is performed by varying machining parameters and experiments are designed using Taguchi's Design of Experiments (DoE), an L_9 Orthogonal Array (OA) is chosen. A hybrid Taguchi–Grey relational approach is used to determine the optimum parameters over measured responses flank wear, roughness, and material removed. Analysis of Variance (ANOVA) result shows that the depth of cut is the influential parameter that contributes toward output responses. A metaheuristic evolutionary algorithm nondominated sorting genetic algorithm (NSGA-II) is applied to optimize the machining parameters for minimizing wear and maximizing metal removal. Experiments with optimum conditions show a better improvement in the output conditions.

Keywords. Aluminum MMC; Taguchi's technique; Grey relational analysis; NSGA-II; ANOVA; Pareto front.

1. Introduction

Composite materials are heterogeneous solids that consist of two or more materials, which are different, metallurgically and mechanically bonded for the purpose of rectifying the weakness in one material with the better properties of another material [1]. The materials that were added to form the composite retain their identity and maintain their properties and characteristics. To suit the varying needs of applications requiring materials with enhanced properties at lighter weight for application in aerospace and automotive fields, novel materials reinforced with ceramic particles were developed. However, the performances of these composites depend on the matrix material, processing techniques, type of reinforcement, and the processing parameters [2]. Aluminum-based metal matrix composites (MMCs) were widely used owing to their light weight, excellent mechanical properties, and higher wear resistance. Plastic deformation resulting in the aluminum metal matrix is reduced by the reinforcements used such as SiC, B_4C, TiC, and Al_2O_3 which is examined through the wear behavior of the composite [3].

Owing to high strength, wear resistance, impact strength, and stiffness, ceramic particles reinforced in metal matrix are becoming attractive materials with increasing applications in automotive industries, aerospace industries, and also in sports equipments. Owing to favorable and enhanced mechanical properties, these particles reinforced with MMCs are used more among the modern advanced composite materials. Reinforcement of silicon carbide particles in the aluminum matrix improves the heat resistance, tensile strength, hardness, and brittleness [4]. With the addition of SiC particles, the machining characteristics change abruptly, producing different chips than that of machining aluminum. High surface roughness and higher tool wear are common during machining Al–SiC MMCs, because of built-up-edge chips favored by high feeds and lower speeds. Machining of MMCs results in excessive wear on tools and roughness on workpieces due to the presence of ceramic reinforcing materials in metal matrix. Hence, tools selected for machining should resist the abrasive wear action of these ceramics. High-speed steels cannot be used for machining because of their poor behavior and therefore advanced tool materials such as cemented carbide, PCD, and cermets were chosen. Among these tool materials, carbides cost lesser than cermets and

*For correspondence

PCDs and, hence, cemented carbide cutting tools are chosen to improve productivity at lower cost. In this aspect, basic machinability tests have to be performed to determine the cutting conditions that suit the usage of carbide tools in machining ceramic particles-reinforced MMCs [5].

To understand the performance and behavior of the prepared composite, mechanical properties and wear behavior can be determined. Powder Metallurgy (P/M) technique is a rapidly evolving technology that embraces most of the metallic and alloy materials. P/M is a highly reliable method for producing ferrous and nonferrous parts. Mostly, high-purity aluminum has been used as matrix to understand the reinforcement and matrix interface relationship, since the impurities that may be present in the base matrix material may influence the interface during the fabrication of the composite. For this purpose, 99.85% pure aluminum is chosen as the matrix material. Copper is one of the best alloying elements added to aluminum in order to increase the conductivity and to increase the strength of the composite. Silicon carbide, a ceramic particulate material, was added to the composite to increase its hardness, strength, and wear resistance.

Pal *et al* [6] prepared Al–Cu–Mg alloy composite with various volume fractions of SiC through P/M process and studied the age-hardening kinetics and indicated that greater dissolution and lower spacing of interparticles had shown better hardness. Rajmohan *et al* [7] investigated the dry sliding wear behavior and the mechanical behavior of Al356 reinforced with mica and ceramic particles and achieved better hardness and strength with 10% addition of SiC and 3% addition of mica, and wear properties increased with mica addition. Shorowordi *et al* [8] developed Al MMCs reinforced with three ceramic particles by different volume fractions by hot extrusion process following stir casting and observed that interfacial bonding tends to improve with reinforcement of B_4C than Al_2O_3 and SiC reinforcements.

Rajaram *et al* [9] studied Al–Si–Cu/graphite MMCs mechanical properties prepared by stir casting technique and determined that composite tensile strength is more than its parent alloy but for different strain rates the elongation of parent alloy is more than its composite counterpart. Senthilkumar *et al* [10] investigated mechanical properties of epoxy polymer reinforced with aluminum oxide particles through fatigue analysis and investigated the distribution of particulates inside the matrix using optical microscope. Pawade and Joshi [11] aimed to minimize cutting forces and roughness through the application of Taguchi–Grey relational analysis (GRA) and showed that the depth of cut is a significant one over the multiple responses on 95% CI. Senthilkumar and Tamizharasan [12] optimized the cutting tool geometry using Taguchi's technique considering multiple performances of maximum MRR and minimum roughness and wear and determined the significant contributions using Analysis of Variance (ANOVA).

Yang and Natarajan [13] solved the multiple responses turning problem by applying differential evolution algorithm and nondominated sorting genetic algorithm (NSGA-II) toward reducing tool wear and improving MRR and reported the comparison of the results obtained from the two techniques used. Srinivas and Deb [14] applied speciation and niche method in Goldberg's notion using genetic algorithm with nondominating sorting technique toward fining pareto-optimal front simultaneously and suggested that the algorithm can be used for more difficult and higher-dimensional multi-objective problems for better results. Palanikumar *et al* [15] applied NSGA-II for investigating the machinability evaluation of GFRP composites over multiple performances and developed second-order regression models to determine a nondominated solution for optimizing the conditions.

In this work, aluminum-based MMC is fabricated via P/M technique, consisting of Al–4%Cu–7.5%SiC composition to study its machinability behavior during turning the MMC with uncoated tungsten carbide cutting tool. Mechanical properties were determined for the MMC to study its performance and the micrograph is studied through scanning electron microscope (SEM) to visualize the distribution of reinforced materials inside the aluminum matrix. Taguchi's Design of Experiments (DoE) is applied to design the experiments and a hybrid Taguchi–GRA is applied toward optimizing multiple characteristics flank wear of the carbide tool, surface roughness on workpiece, and MRR. An evolutionary metaheuristic optimization technique, NSGA-II developed in Matlab code is also used to determine the optimum conditions for the determined multiple characteristics with consideration of surface roughness as constraint.

2. Material selection

The base material chosen for the preparation of MMC is aluminum, copper as a secondary material, and silicon carbide to reinforce the matrix. Aluminum is chosen to reduce the weight of the material, copper is added to increase the thermal conductivity of the material, and silicon carbide is added to improve the strength and hardness of the MMC. The base materials SEM are shown in figure 1.

The cutting tool insert chosen for machining the P/M MMC is uncoated cemented carbide of ISO designation TNMG 120404, as shown in figure 2. The SEM image of carbide cutting insert shows the particles of tungsten carbide (WC) that are predominant. The structure consists of varying composition of tungsten carbide and titanium carbide phases of solid solution. Voids present in the structure are seen as black area and cobalt solid solution is observed between the voids, which are used as a binder. The marginal dendritic solid solution of cobalt is seen at the extreme right.

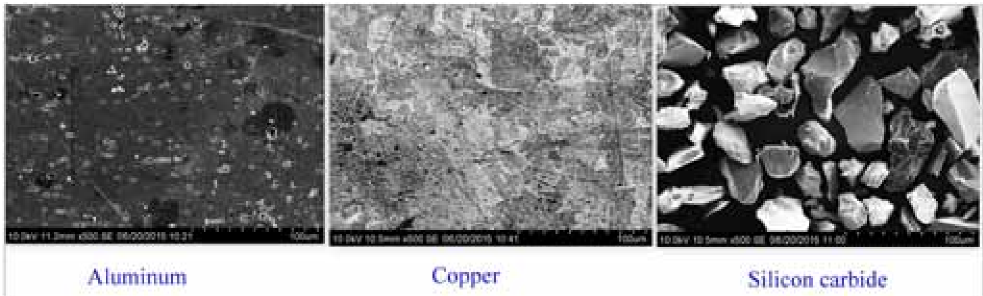

Figure 1. SEM image of base materials.

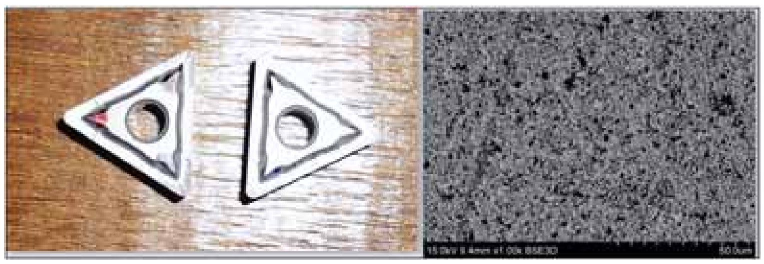

Figure 2. Cutting tool insert used and its SEM image.

3. Techniques applied for experimentation and analysis

3.1 *Powder metallurgy route*

The process of P/M consists of identifying the required base material, weighing the ingredients in proper proportions by volume fractions, and then mixing the materials well for uniformity. The mixed powders were compacted at 20 tons in a closed die. Compacting the mixed materials was carried out using a die for the required shape and size in a universal testing machine. The compacted sample was sintered at 500 °C for 3 hours. The furnace was maintained with nitrogen atmosphere of 0.5 liters per minute. Figure 3 outlines the procedure of P/M process used in the preparation of the composite material as a flow chart.

The microstructure of the P/M specimen, shown in figure 4, shows some unfused/undissolved free copper in the matrix. The percentage of free copper is about 0.6% in volume. The rest of the matrix shows fine fused $Cu–Al_2$ in aluminum solid solution. The particles of SiC present are uniformly distributed in the matrix. The SiC particles are shown as dark gray particles in the Al–Cu matrix.

The mechanical properties of the cast Al–4%Cu–7.5%SiC were characterized by means of hardness test, compression test, and wear test. The hardness value is 42.93 HR, when done with Rockwell hardness test (T-Scale) performed with 15 kgf load and with 1/16-inch diameter indenter. The compressive test yields an ultimate strength of 19.96 kN and the ultimate stress as 0.062 kN/mm^2. The wear rate of the MMC obtained from the pin-on-disc apparatus test is 6.82E-8 g/cm. The maximum coefficient of friction and frictional force for the MMC is 0.66 and 1.99 N, and the minimum coefficient of friction and frictional force is 0.13 and 0.4 N, respectively.

3.2 *Design of experiments*

Process parameters were optimized with a powerful tool, Taguchi's DoE [16], making use of special design of orthogonal arrays (OAs) with a minimum number of experiments for evaluating the outputs. Outputs obtained during the experiments are then converted for further evaluation to signal-to-noise (S/N) ratio [17, 18] based on the conditions that it should be minimum or maximum. In this work, experimental array was designed considering feed rate, cutting speed, and depth of cut. These inputs are varied through three levels and the values chosen for level conditions are shown in table 1.

Using Minitab-16, statistical package, for the selected input parameters and their value range, an L_9 is selected from the array selector for three parameters three levels. OA from Taguchi's DoE for varying combinations of machining conditions is shown in table 2.

CNC turning center with two axes is used to conduct the experiments with swing diameter of 350 mm, distance between centers as 600 mm and with maximum spindle speed of 4500 rpm. After completion of the experiments, tool wear at flank face was measured using Mitutoyo make

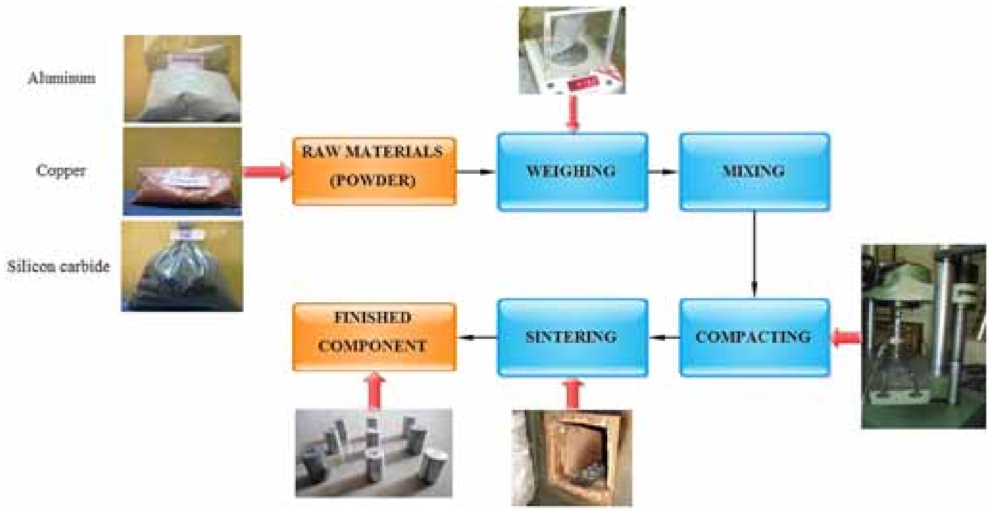

Figure 3. Flow chart of MMC preparation by P/M route.

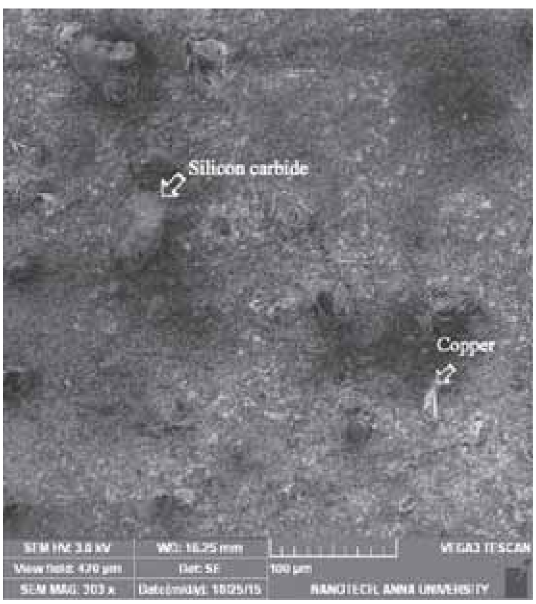

Figure 4. SEM image of P/M MMC.

Tool makers microscope (digital type), with eyepiece magnification of 15×, maximum 13 mm field diameter, 2× objective lens magnification with total magnification of 30×, and maximum working distance of 67 mm. Kosaka Laboratory make Surfcorder SE1200 is used to measure surface roughness in the specimen surface whose specifications were 520 μm and 25 mm in both vertical and horizontal ranges, 0.8 mm cutoff values with Gaussian filter. The rate at which the material is removed from the workpiece is calculated by weighting the workpiece before and after machining; the difference is determined and divided by the time taken for machining. In Taguchi's technique, there are three categories for analyzing the outputs: larger-the-better, nominal-the-better, and smaller-the-better concepts [19]. Process will be more robust against the external noises if the S/N ratio is larger, for undesired output, the chosen category is smaller-the-better. Larger-the-better category is chosen for desired, and for a nominal output, nominal-the-better category is selected.

Minimize (Smaller-the-better):

$$S/N = -10\log\left(\frac{1}{n}\sum_{i=1}^{n} y_i^2\right). \quad (1)$$

Maximize (Larger-the-better):

$$S/N = -10\log\left(\frac{1}{n}\sum_{i=1}^{n} \frac{1}{y_i^2}\right). \quad (2)$$

Nominal-the-better:

$$S/N = 10\log\left(\frac{\bar{y}}{s_y^2}\right) \quad (3)$$

Table 1. Level values of control parameters.

Parameter/level	Notation	Level 1 (−1)	Level 2 (0)	Level 3 (+1)
Cutting speed (m/min)	A	120	150	180
Feed rate (mm/rev)	B	0.05	0.07	0.09
Depth of cut (mm)	C	0.15	0.30	0.45

Table 2. Formulated L_9 inner array.

Trial no.	Coded values			Actual values		
	Cutting speed (m/min)	Feed rate (mm/rev)	Depth of cut (mm)	Cutting speed (m/min)	Feed rate (mm/rev)	Depth of cut (mm)
1	−1	−1	−1	120	0.05	0.15
2	−1	0	0	120	0.07	0.30
3	−1	+1	+1	120	0.09	0.45
4	0	−1	0	150	0.05	0.30
5	0	0	+1	150	0.07	0.45
6	0	+1	−1	150	0.09	0.15
7	+1	−1	+1	180	0.05	0.45
8	+1	0	−1	180	0.07	0.15
9	+1	+1	0	180	0.09	0.30

where y_i represents the values observed experimentally of ith experiment and replications or repetition of experiments is given as n.

3.3 *Grey relational analysis*

Optimization of multiple responses can be simultaneously performed with GRA to find out the optimal levels that consists of many outputs [20–22]. With the meager information available, GRA can judge or evaluate the performances of complex process that involves more than one output. In GRA, the raw data have to be preprocessed into a quantitative index for subsequent analysis [23–25]. Preprocessing raw data involves conversion or raw data into decimal sequence that lies between 0.00 and 1.00, which is useful for comparison. The sequence can be normalized for the condition Higher-the-better as

$$x_i^*(k) = \frac{x_i^0(k) - \min x_i^0(k)}{\max x_i^0(k) - \min x_i^0(k)} \tag{4}$$

x_i^* (k) represents the data sequence after preprocessing, x_i^o (k) represents the original sequence, largest value of x_i^o (k) is max x_i^o (k), smallest value of x_i^o (k) is min x_i^o (k) imply the. Normalizing the data for lower-the-better condition is given as

$$x_i^*(k) = \frac{\max x_i^0(k) - x_i^0(k)}{\max x_i^0(k) - \min x_i^0(k)}. \tag{5}$$

After completing data preprocessing, in order to express a relationship between actual and ideal normalized values, a Grey relational coefficient is determined, as expressed in Eq. (6):

$$\zeta_i(k) = \frac{\Delta_{\min} + \zeta.\Delta_{\max}}{\Delta_{0i}(k) + \zeta.\Delta_{\max}} \tag{6}$$

Δ_{oi} (k) represents the deviation sequence, which is calculated by

$$\Delta_{0i}(k) = \left\| x_0^*(k) - x_i^*(k) \right\| \tag{7}$$

$$\begin{aligned} \Delta_{\max} &= \max_{\forall j \varepsilon i} \max_{\forall k} \left\| x_0^*(k) - x_j^*(k) \right\|, \\ \Delta_{\min} &= \min_{\forall j \varepsilon i} \min_{\forall k} \left\| x_0^*(k) - x_j^*(k) \right\| \end{aligned} \tag{8}$$

ζ is known as identification coefficient: ζ lies between the values 0 and 1. Normally ζ is chosen as 0.5 [26]. Grey relational grade is calculated for optimizing multiple responses by the method of calculating average values of Grey relational coefficient for each response level values, as given in Eq. (9).

$$\gamma_i = \frac{1}{n} \sum_{k=1}^{n} {}_i\zeta_i(k). \tag{9}$$

3.4 *Empirical modeling and analysis of variance*

Evaluating the difference between the set of scores is performed by means of ANOVA, which can be applied over the raw data that is used to divide the total measured variance into different component parts [27]. The total measured variance of the data set is the variance of individual data scores obtained while measuring over the dependent individual variable. ANOVA is necessary to find out the input parameters that have significant influence over the measured responses and amount of contribution toward it.

Regression models have a strong relationship with experimental design to emphasize the importance of quantitative expression of results by means of empirical modeling for better implementation, interpretation, and understanding [28]. Experimental models, appearing more complex in nature, can be analyzed by means of multiple linear or nonlinear regression techniques. In this analysis, a first-order model is formulated for the measured output responses in terms of input parameters as shown in Eq. (10):

$$Y = a_0 + \sum_{i=1}^{n} a_i X_i + \sum_{i=1}^{n} a_{ij} X_i Xj + e. \qquad (10)$$

3.5 *Nondominated sorting genetic algorithm*

Kalyanmoy Deb proposed NSGA-II [29–32], which is the new revised format of the previous version of NSGA-I. The updated version is more efficient computationally by the usage of elitism and crowded method of comparison operator. In NSGA-II, elitist mechanism combines the best offspring from the best parents, which assures the preservation of best global solutions. The procedure for sorting nondominated solution is faster in this version. Most importantly, this new version does not require any parameter to be tuned, making this algorithm user independent. Figure 5 shows how the elites are preserved in NSGA-II.

During preserving the elites, NSGA-II develops a competing population of individuals, then ranks it according to its nondomination level values, and then sorts it out thereby creating a new pool of better offspring for the next stage, thus producing a new combined pool of population by combining the parents and offspring [33]. By adding a crowding distance to each member of the newly generated population, NSGA-II then conducts niching. To explore the fitness landscape and to keep each individual to stay at some crowding distance apart from other individuals, NSGA-II uses crowding distance in its selection operator [34]. Figure 6 outlines the improved NSGA-II as a flowchart [30].

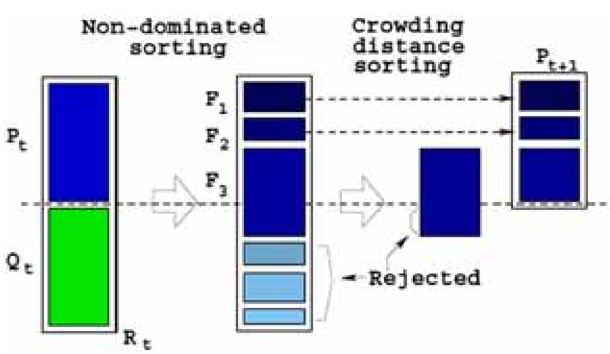

Figure 5. Preservation of elites in NSGA-II.

In the first step, random population of parents P_o is developed and is sorted on nondomination basis and to reduce the complexity in computation, a special procedure of $O(MN^2)$ is done. A fitness value of nondominated level (normally 1) is assigned to each of the solution, thereby assuming fitness minimization. Child population Q_o of size N is created using binary tournament method, crossover and mutation operators.

Initially to ensure elitism, to compare the parent solutions with child population, a population combining parents and offspring is formed by $R_t = P_t U Q_t$. The size of the population R_t is $2N$. Then, according to nondominated fronts sorting of population, R_t is done. The working of NSGA-II algorithm is as follows.

From the chosen population, solutions obtained from the nondominated front are added to develop a new population of parents Pt+1 until the population size is reached. Crowding distance is calculated from the individuals of nondominated fronts. Comparing the crowded distance, sorting of solutions are carried out for N points. Criteria used by crowding distance comparison uses the relationship as: In α_n relationship ith solution is better than jth solution if the condition $(i_{\text{distance}} > j_{\text{distance}})$) and $(i_{\text{rank}} \le j_{\text{rank}})$ is reached, thereby importance is given to solutions derived from search space having less-dense regions to select from R_t, which forms the new population P_t+1. To apply the operators, such as binary tournament selection method, crossover, and mutation for creating new population of Q_t+1, this population is used. This procedure should be continued for the number of generations selected. The parameter values used during simulation of iteration of NSGA-II algorithm is real variable type with population size of 100, 0.9 crossover probability, and mutation probability of real parameter is 1, SBX parameter value of 10, mutation parameter value of 100 with number of iterations/generations of 100.

4. Results and discussion

With the experimental setup in CNC turning center, experiments were conducted as per the designed OA. During the turning process, a separate workpiece and

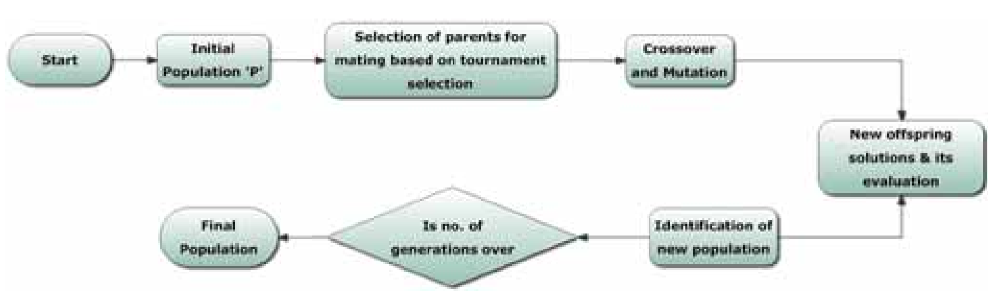

Figure 6. NSGA-II flow chart.

Table 3. Measured output responses.

	Flank wear (mm)			Surface roughness (µm)			MRR (g/min)		
Trial no.	R_1	R_2	Average	R_1	R_2	Average	R_1	R_2	Average
1	0.254	0.244	0.249	0.321	0.331	0.326	1.746	1.756	1.751
2	0.291	0.301	0.296	0.404	0.416	0.410	4.026	4.014	4.020
3	0.487	0.479	0.483	0.719	0.701	0.710	7.826	7.842	7.834
4	0.286	0.282	0.284	0.381	0.359	0.370	4.123	4.097	4.110
5	0.742	0.752	0.747	0.498	0.488	0.493	6.272	6.254	6.263
6	0.299	0.305	0.302	0.558	0.542	0.550	3.581	3.591	3.586
7	0.923	0.909	0.916	0.411	0.433	0.422	5.178	5.208	5.193
8	0.287	0.295	0.291	0.446	0.466	0.456	3.227	3.213	3.220
9	0.416	0.424	0.420	0.498	0.514	0.506	6.768	6.776	6.772

cutting tool insert is used for every experiment and the corresponding output responses were measured, which is provided in table 3. The experiments are conducted twice R_1 and R_2 (replications) in order to minimize the experimental error and the average of the values are taken for analysis.

Observations made from the experimental results show that an increase in cutting speed increases flank wear and MRR increases with decrease in surface roughness. Excessive tool wear is experienced along with severe deformation rate with larger cutting speeds [35]. With increase in flank wear, cutting forces also increases. Selection of higher depth of cut and feed rates will result in unexpected effect on surface quality [36]. Higher cutting speed tends to improve the surface finish, whereas poor surface finish can be observed with lower cutting speed, which leads to the fracturing of developed chips leading to surface imperfections. Thermal softening occurs at higher cutting speeds, which removes the built-up edge on the tool thereby reducing the surface roughness [37]. With lower feed rates, lower surface roughness is observed due to the less fracture rate in the surface. When the feed rate is increased, cutting forces increases, chatter is observed and machining at faster rate results in incompleteness. When depth of cut increases, built-up edge on cutting tool increases due to high pressure between the tool and workpiece [38]. With increase in feed rate, flank wear reduces but at the same time higher material is removed from the workpiece, thereby making the surface wavy. All the outputs MRR, surface roughness, and flank wear increase when the depth of cut is increased. Tool wear of the cemented carbide tools increases when cutting speeds are increased, owing to the abrasion action of the chips on the flank face of tool insert [39]. Flank wear surfaces were produced due to the abrasion action of the produced chips. Resistance to abrasion is related to tool hardness [40]. Increasing the depth of cut does not make any sense toward the tool wear, so it is suggested to utilize higher depth of cuts to achieve high production rates without any tool wears. Increasing the feed rate for a specific amount of material removed from the stock reduced the tool wear. Hence, an effective way to improve material removal and tool life is to increase the feed rate.

Exploring the potential relationship that exists between three variables is possible with contour plots, displaying the three-dimensional relationship in a two-dimensional way with variables plotted on x and y axes and response values represented by contour lines. Typical applications of these contour plots are useful in determining the settings of parameters that will minimize or maximize the measured responses.

Determination of variable settings that will result in a predetermined response variable target value can be visualized through these contour plots. The information that can be derived from the contour plots includes the significance of interactions between the two variables and best data setting for obtaining the better output response. The influence of control variables on the output responses is shown in figures 7, 8, 9. The contour plot of variables over the responses is also shown, from which the desired combination of input variables can be chosen for a specific target value of response.

For optimizing the average value of measured output responses, hybrid Taguchi–Grey technique is applied to convert the individual single objectives into a multi-objective problem [41]. Initially, with the nature of measured responses, S/N ratio formulae for smaller-the-better or larger-the-better of Taguchi's technique are applied to the output values to determine the individual S/N ratio for responses. Lower values of flank wear at tool face and roughness at workpiece surface are desirable, for that Eq. (1) is applied. Higher material removal is desirable, and hence Eq. (2) is applied. After determining the S/N

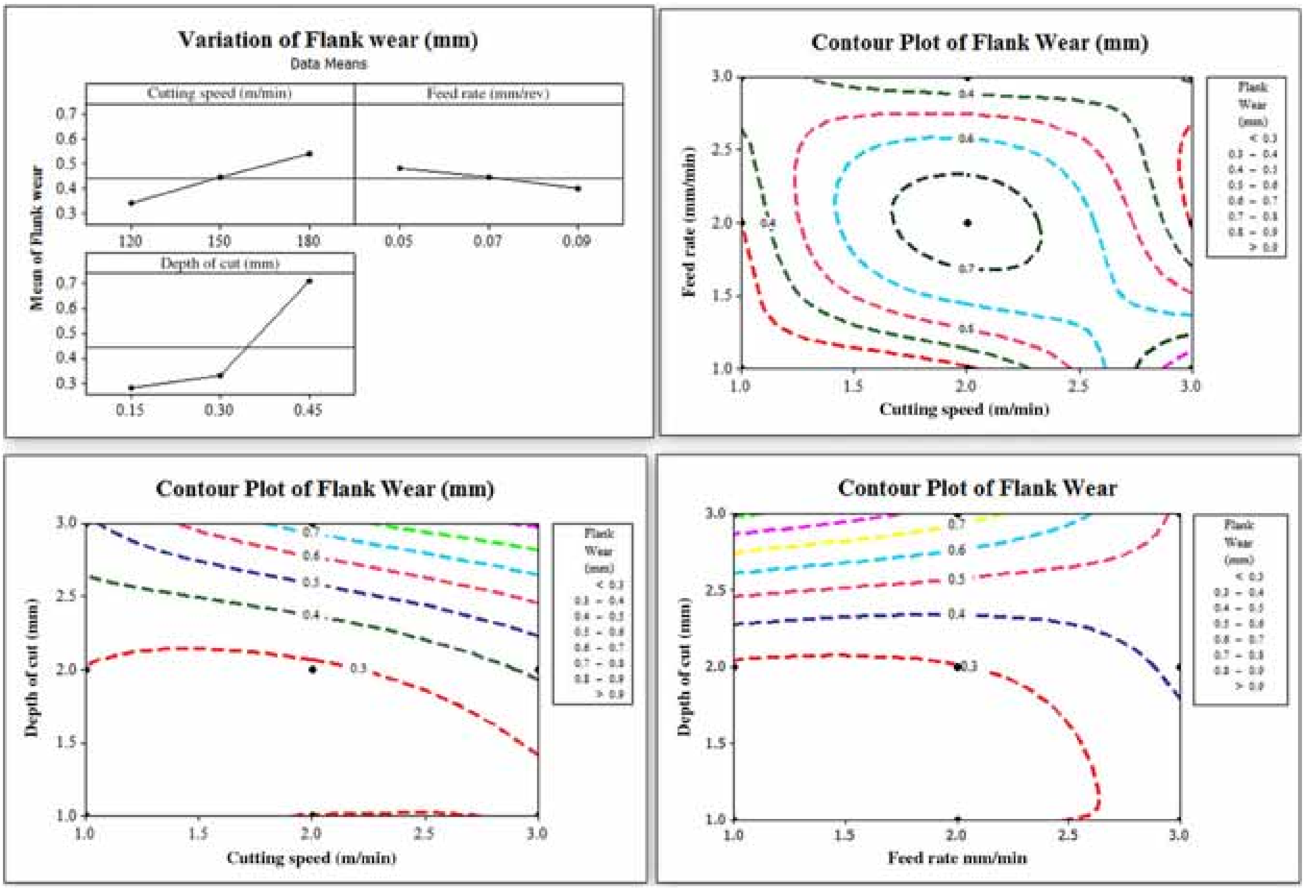

Figure 7. Influence of control variables on flank wear.

ratio, the values have to be normalized based on the lower or higher desirable concept of GRA, as given in Eqs. (4) and (5), which are given in table 4.

After the normalizing procedure, the deviation sequence of the responses is determined. A Grey relational coefficient is determined for individual responses and then a common Grey relational grade has to be calculated in order to convert the single objective optimization into multi-objective optimization by considering the average values of individual Grey coefficients of outputs. Ranking is given based on the higher Grey grade and experiment number 3 ranks first and experiment number 1 ranks last (table 5).

To derive the response table of Grey grade, shown in table 6, average values of each parameter level is considered and from that the optimum conditions are evolved by choosing the level values with larger Grey grade. The best/optimal parameter levels are identified from the response table as 180 m/min cutting speed; 0.09 mm/rev feed rate, and 0.45 mm depth of cut, represented as $A_3B_3C_3$. Response plot of Grey relational grade is drawn based on response table, which is shown in figure 10.

Influence of parameters on the output response can be easily studied by means of the linear graph, also known as interaction plot. Figure 11 shows the influence of various inputs over the output Grey relational grade. If the relationship between two input parameters over the output parameter is represented as parallel lines, then it is concluded that no interaction exists between the two inputs. If their relationship is represented as nonparallel lines, then it is concluded that a prominent relationship exists between the two inputs. From the interaction plot drawn, it is obvious that a significant interaction exists between the feed rate and all level values of cutting speed. In between

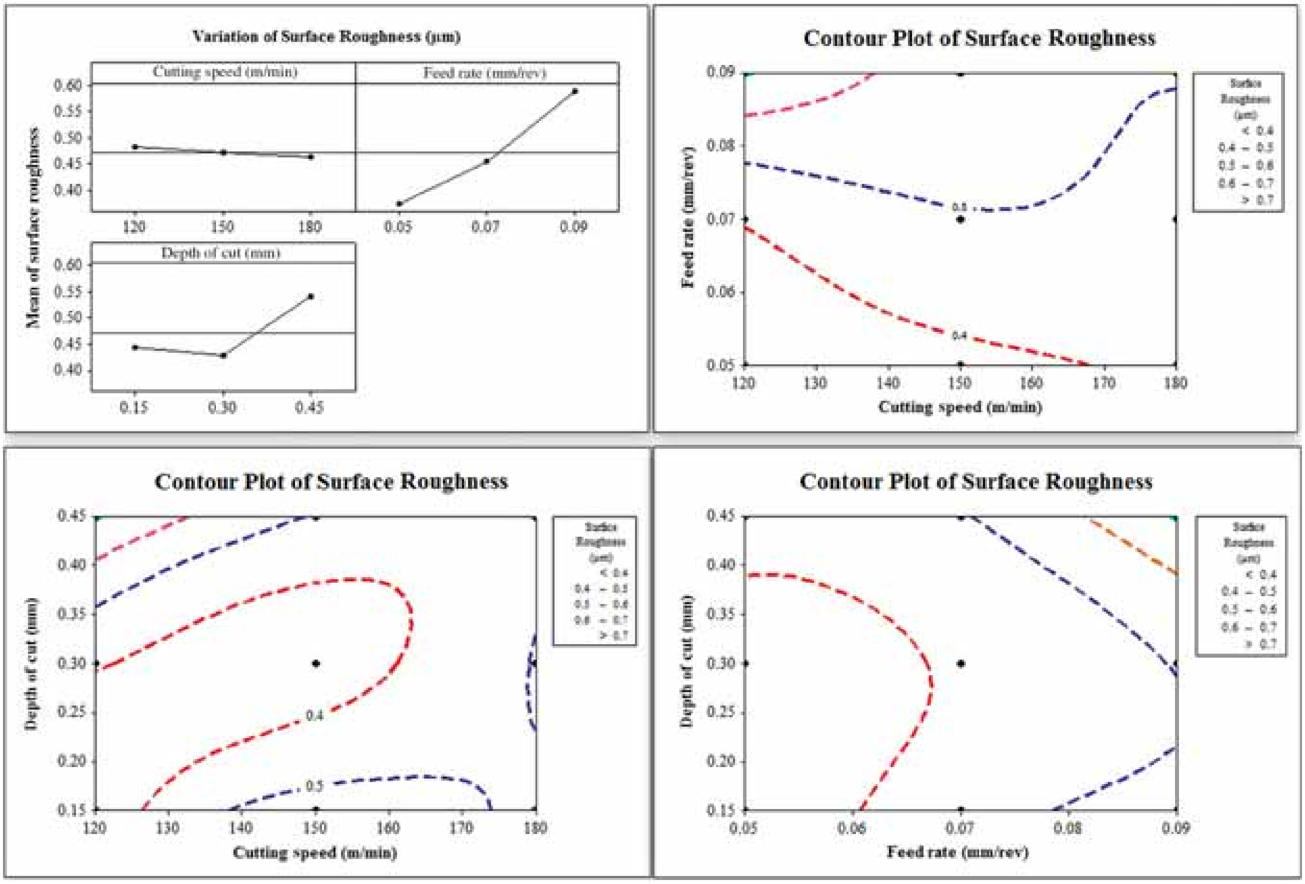

Figure 8. Influence of control variables on surface roughness.

depth of cut and chosen values of cutting speed, considerable amount of interaction exist. But in between depth of cut and feed rate no interaction effect exists.

The statistical way of determining the significant parameter and quantification of its contribution toward the output is ANOVA. From the ANOVA we can determine the most influential parameter that contributes toward the output, by controlling that parameter the outputs can be controlled. Results of ANOVA method are given in table 7.

From the ANOVA table of S = 0.0225191, R^2 value = 99.53% and R^2 (Adj) = 98.13%, it is understood that the model developed is better since the R^2 and R^2 (Adj) values are close to 100% and are closer to each other. Nearly 77.67% contribution by depth of cut makes it the most influential parameter, followed by 20.12% of feed rate and the contribution of cutting speed is negligible since it contributes only by 1.74%. The error obtained during the analysis is 0.47%.

4.1 *Validation experiment for Taguchi–Grey analysis*

On the basis of identified optimal input parameters, a validation experiment is performed with the said experimental setup to validate the results. The outputs obtained are flank wear of 0.359 mm, 0.418 µm surface roughness, and 5.124 g/min of material removal, which are considerably better than that of the values observed and recorded. With the measured output of confirmation experiment, reduction in flank wear by 18.98%, surface roughness by 11.34% with an increase in MRR by 7.88% is observed. From the results obtained, the efficiency of the Taguchi–GRA technique is better understood.

4.2 *Development of empirical models*

Multiple nonlinear first-order regression models are developed for individual measured responses using statistical

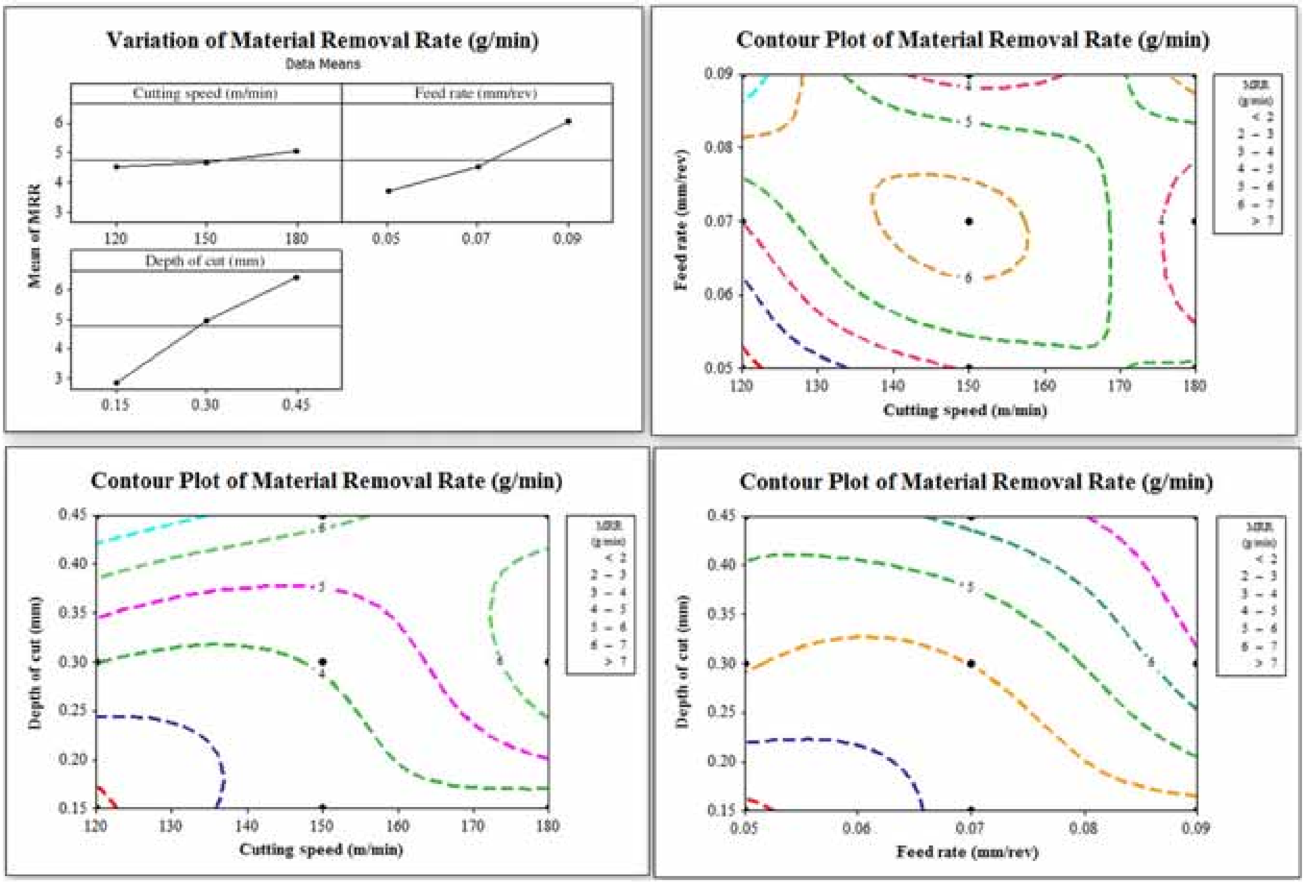

Figure 9. Influence of control variables on MRR.

Table 4. Calculated S/N ratio and GRA normalizing sequence of responses.

	S/N ratio			Normalizing sequence		
Trial no.	Flank wear	Surface roughness	MRR	Flank wear	Surface roughness	MRR
1	12.076	9.736	4.866	0.000	0.000	0.000
2	10.574	7.744	12.085	0.133	0.295	0.555
3	6.321	2.975	17.880	0.509	1.000	1.000
4	10.934	8.636	12.277	0.101	0.163	0.569
5	2.534	6.143	15.936	0.843	0.531	0.851
6	10.400	5.193	11.092	0.148	0.672	0.478
7	0.762	7.494	14.308	1.000	0.332	0.726
8	10.722	6.821	10.157	0.120	0.431	0.407
9	7.535	5.917	16.614	0.401	0.565	0.903

Table 5. GRA deviation sequence and Grey grade of responses.

	Deviation sequence			Grey relational coefficient				
Trial no.	Flank wear	Surface roughness	MRR	Flank wear	Surface Roughness	MRR	Grey relational grade	Ranking
1	1.000	1.000	1.000	0.333	0.333	0.333	0.333	9
2	0.867	0.705	0.445	0.366	0.415	0.529	0.436	6
3	0.491	0.000	0.000	0.504	1.000	1.000	0.835	1
4	0.899	0.837	0.431	0.357	0.374	0.537	0.423	8
5	0.157	0.469	0.149	0.762	0.516	0.770	0.683	3
6	0.852	0.328	0.522	0.370	0.604	0.489	0.488	5
7	0.000	0.668	0.274	1.000	0.428	0.646	0.691	2
8	0.880	0.569	0.593	0.362	0.468	0.457	0.429	7
9	0.599	0.435	0.097	0.455	0.535	0.837	0.609	4

Table 6. Response table for weighted Grey grade.

Level/parameter	Cutting speed	Feed rate	Depth of cut
Level 1	0.535	0.482	0.417
Level 2	0.531	0.516	0.489
Level 3	**0.576**	**0.644**	**0.736**

Bold values indicate the maximum values that corresponds to the optimum condition

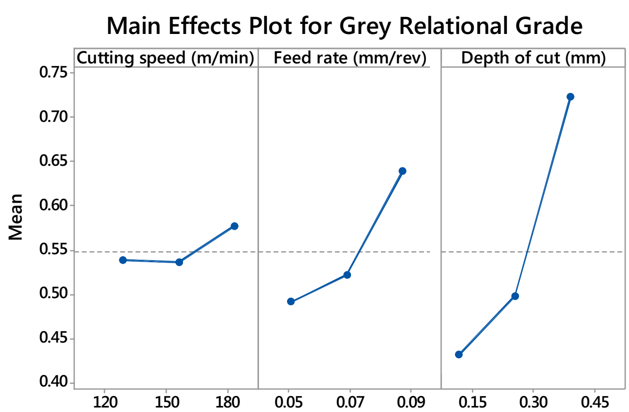

Figure 10. Response plot for Grey relational grade.

software Minitab-17. The fitted model empirical equations for quality characteristics are given in Eqs. (11)–(13).

$$Flank\ wear = -0.665746 + 0.00603016\,speed + 26.8381\,feed - 5.44683\,depth - 0.19\,speed*feed + 0.0374603\,speed*depth + 12.8095\,feed*depth \tag{11}$$

$$Surface\ roughness = -1.05356 + 0.0102437\,speed + 24\,feed - 2.31683\,depth - 0.16119\,speed*feed + 0.00577778\,speed*depth + 20.7619\,feed*depth \tag{12}$$

$$MRR = 0.122079 + 0.00526587\,speed - 32.3381\,feed + 0.659365\,depth + 0.227381\,speed - feed - 0.00990476\,speed*depth + 188.667\,feed*depth. \tag{13}$$

The plot of normal probability obtained during developing first-order nonlinear regression models for flank wear, MRR, and surface roughness is shown in figure 12. The residuals of probability plot for output responses follow a straight line with the values situated nearby and no evidence of skewness, outliers, nonnormality, and unidentified existing of variables are seen, which provides as better fit. The surface plot shows the relationship between the three outputs: higher removal of material facilitates wear and roughness.

4.3 *Application of NSGA-II algorithm*

The objective of this present investigation and analysis is to lower the wear at flank face and to increase the amount of material removed with the aim of keeping the surface roughness within a desired value, that is, minimize flank wear, maximize MRR with surface roughness as constraint. The nontraditional metaheuristic algorithm used is NSGA-II. The formulation of objective function is as follows:

Objective function formulation: Minimize (flank wear) + Maximize (MRR).
Constraint: Roughness $\leq$ 0.3 µm.

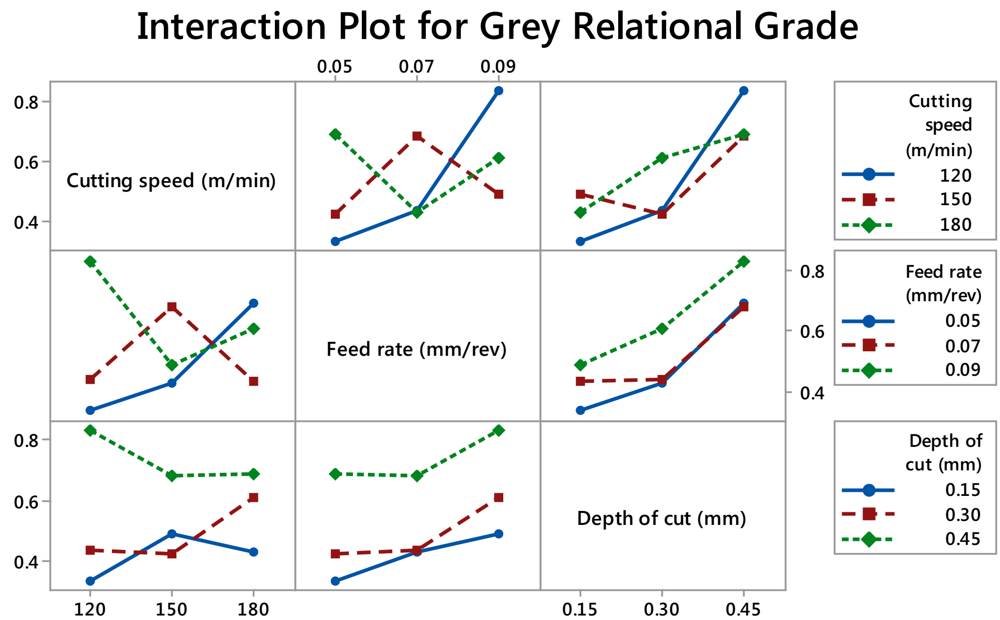

Figure 11. Interaction plot for Grey relational grade.

Table 7. Analysis of variance for Grey grade.

Parameter	DF	Seq SS	Adj MS	F	P	% Contribution
Cutting speed	2	0.003772	0.001886	3.72	0.212	1.74
Feed rate	2	0.043654	0.021827	43.04	0.023	20.12
Depth of cut	2	0.168476	0.084238	166.11	0.006	**77.67**
Error	2	0.001014	0.000507			0.47
Total	8	0.216916				100

Bold value indicates the most significant factor (depth of cut) that contributes by an higher percentage

Equal weightage (50%) is considered for flank wear and MRR in this work. Maximization problem is converted in to minimization problem by negating the maximization equation; the objective function can be reformulated as

Objective function = (50% flank wear) – (50% MRR);
Subject to the constraint: Surface roughness $\leq$ 0.3 µm.
The lower limit and upper limit of the parametric constraints are given as
120 $\leq$ cutting speed $\leq$ 180
0.05 $\leq$ feed rate $\leq$ 0.09
0.15 $\leq$ depth of cut $\leq$ 0.45

From the simulation results obtained from NSGA-II, the optimum machining conditions obtained are: 136 m/min of cutting speed, 0.057 mm/rev of feed rate, and 0.45 mm of depth of cut. The predicted output responses during the optimization procedure are: flank wear of 0.378 mm, MRR of 5.231 g/min, and surface roughness of 0.2995 µm, which is well within the set constraint value.

The combined objective function obtained during simulation for all iterations is shown in figure 13. It is observed that initially the objective function is close to higher and as the iteration progresses, the value of objective function converges toward the lower value. It is also observed that the convergence of combined objective function is faster toward the final optimum result.

The variation of cutting speed during each iteration of the simulation process is presented in figure 14. From the graph, initially the cutting speed is around 123 m/min, and as the simulation continues, cutting speed settles down to 136 m/min.

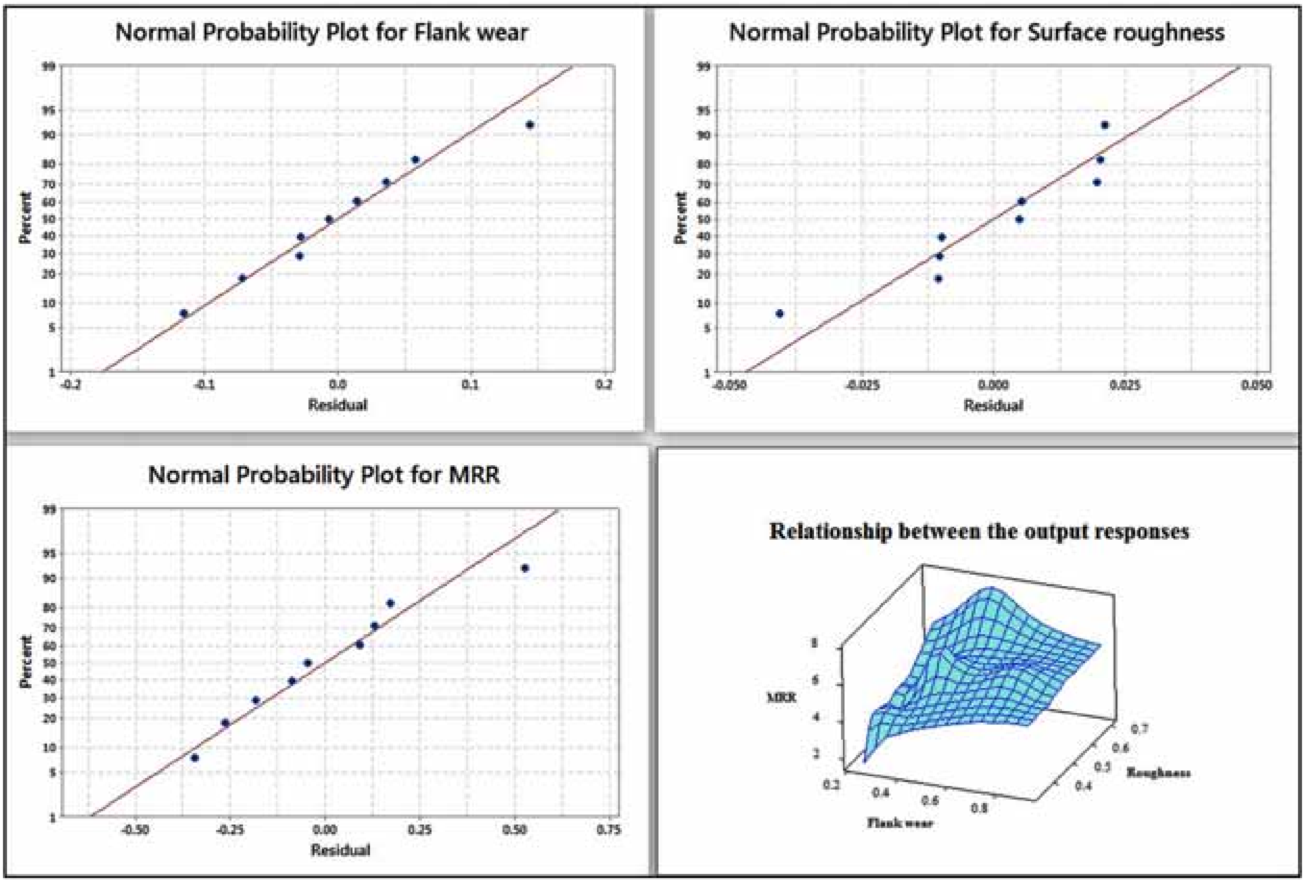

Figure 12. Normal probability plot for output responses and its surface plot.

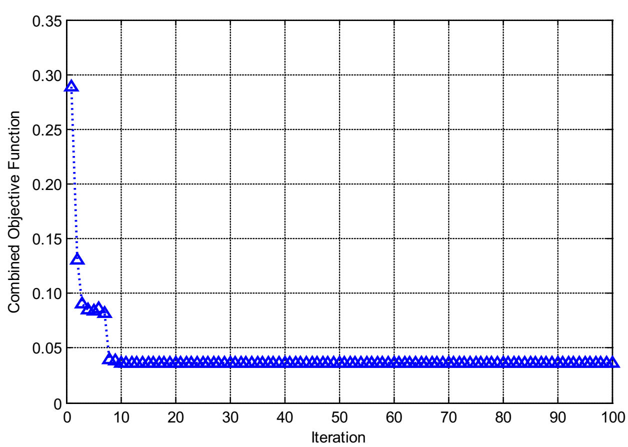

Figure 13. Variation of objective function with iterations.

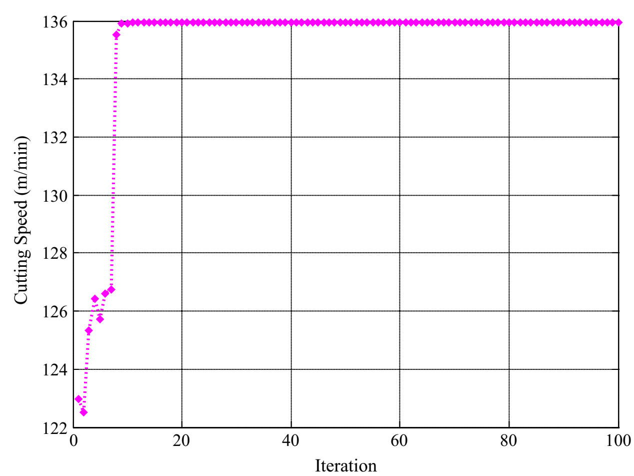

Figure 14. Variation of cutting speed with iterations.

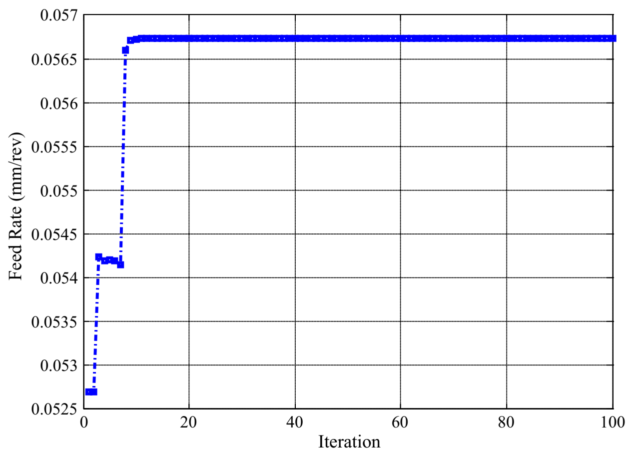

Figure 15. Variation of feed rate with iterations.

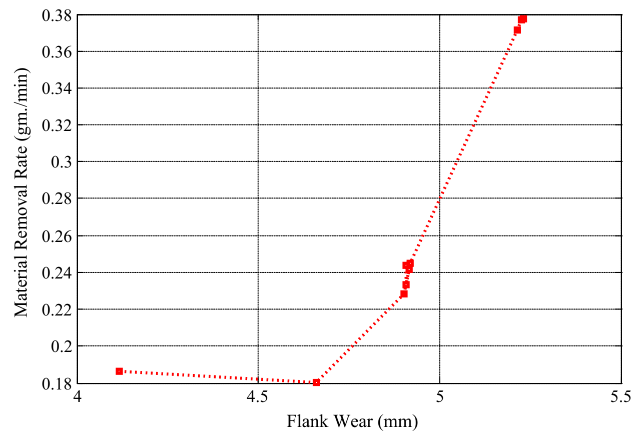

Figure 17. Pareto-optimal front developed for objective function.

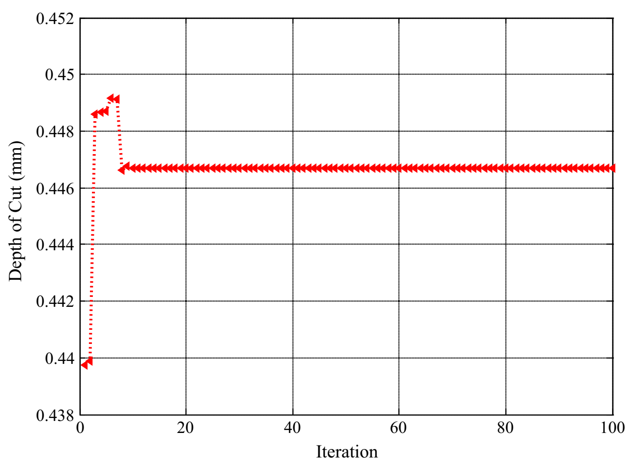

Figure 16. Variation of depth of cut with iterations.

The varying values of feed rate while simulating NSGA-II are given in figure 15. It is observed that the feed rate varies from 0.0527 and finally settles around 0.0567 mm/rev, which is on the lower side of the chosen limits.

The variation of depth of cut value obtained during iteration of algorithm is given in figure 16. During the iterations, the depth of cut varies between 0.44 and 0.49 mm and finally settles around 0.4467 mm, which is on the higher side of the parametric limits.

The nondominated solution set in the entire search space is the pareto-optimal front [42]. Many solutions that trade-off between the two chosen objectives, namely, minimization of flank wear and maximization of MRR, are shown in figure 17. In nondominated solution, one solution will be better than the other solution in both the objectives, whereas for other condition, one solution will be better than the other solution in one objective, and it can be a wrong solution for the another objective.

Table 8. Predicted and experimental results of NSGA-II.

	Flank wear (mm)	Surface roughness (μm)	MRR (g/min)
Predicted	0.378	0.299	5.231
Experimental	0.397	0.391	5.617
% Deviation	4.79	23.40	6.87

4.4 *Validation experiment for NSGA-II*

Another validation experiment is carried out with optimum parametric values obtained from the metaheuristic algorithm with input values of 136 m/min cutting speed, 0.057 mm/rev feed rate, and 0.45 mm depth of cut. The measured outputs are tabulated in table 8.

From the validation experimental results, observation highlights that simulation results of NSGA-II are nearer to the predicted values thereby a better optimization is possible with the algorithm. The flank wear at the cutting insert flank face and profile of surface roughness of machined surface obtained from the validation experiment of the P/M MMC specimen is given in figure 18. The surface roughness profile shows a better profile, which varies very low with respect to the mean line.

5. Conclusions

The conclusions derived by applying an hybrid Taguchi–GRA and an metaheuristic nontraditional algorithm NSGA-II during machining P/M prepared Al–4%Cu–7.5%SiC with uncoated cemented carbide inserts are as follows:

- The optimum machining condition obtained with application of hybrid Taguchi–GRA is cutting speed: 180 m/min, feed rate: 0.09 mm/rev, and depth of cut: 0.45 mm.

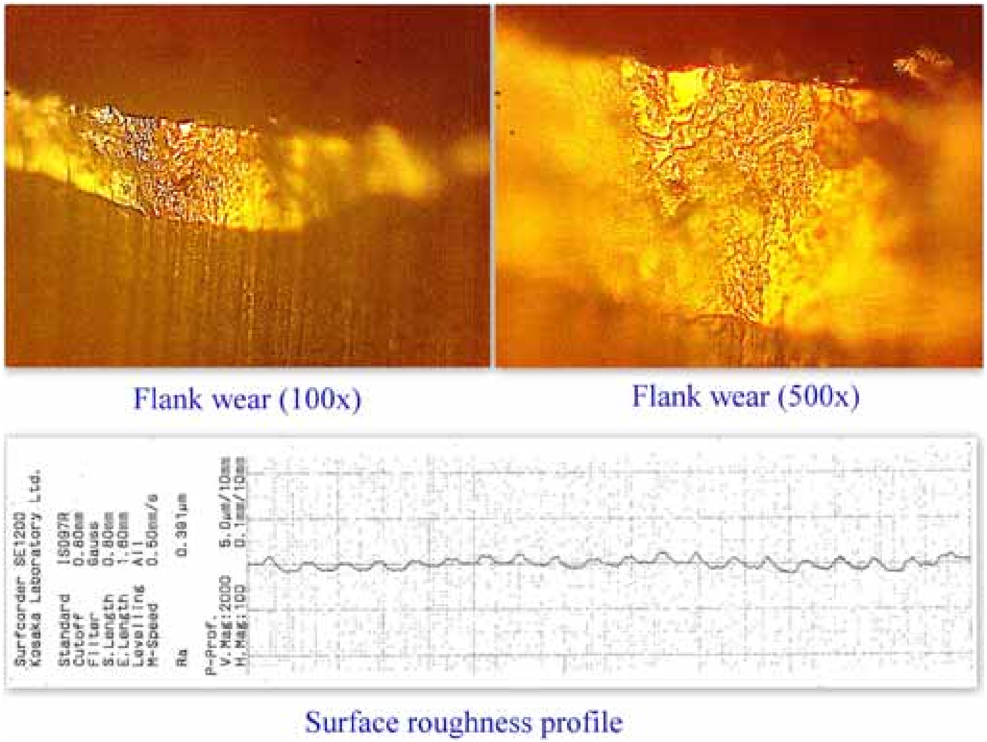

Figure 18. Tool wear and surface roughness profile of optimum condition.

- A significant relationship/interaction exists between the feed rate and cutting speed and also between depth of cut and cutting speed, when all the selected level values of cutting speed is considered. But no interaction exists between feed rate and depth of cut.
- Statistical results of ANOVA outlines that 77.67% of the process is mainly controlled by the parameter depth of cut and 20.12% process is controlled by feed rate. With meager contribution, cutting speed does not show any influence on the output of the machining process.
- Machining with optimum condition reached with hybrid Taguchi–GRA approach reduces flank wear by 18.98% and surface roughness by 11.34% with an increase in MRR by 7.88%.
- Using Minitab-17 statistical software, nonlinear empirical models are developed, which are fed into the NSGA-II algorithm. The optimum machining parameters obtained from NSGA-II are cutting speed of 136 m/min, depth of cut of 0.45 mm, and feed rate of 0.057 mm/rev.
- From the confirmation experimental results of NSGA-II, observation proves that NSGA-II simulation results are well nearer to the predicted values, thereby a better optimization is possible with the algorithm. Pareto front developed will be useful in effective choosing of parameters for maximum MRR and minimum flank wear.

References

[1] DeGarmo E P, Black J T and Ronald A Kohser 2008 *Non-metallic materials: Plastics, elastomers, ceramics, and composites, materials and processes in manufacturing*. Tenth edition, Wiley, New York

[2] Akhlaghi F, Lajevardi A and Maghanaki H M 2004 Effects of casting temperature on the microstructure and wear resistance of compocast A356/SiCp composites: A comparison between SS and SL routes. *J. Mater. Process. Technol.* 155–156: 1874–1880

[3] Ipek R 2005 Adhesive wear behaviour of B_4C and SiC reinforced 4147 Al matrix composites (Al/B_4C–Al/SiC). *J. Mater. Process. Technol*. 162–163: 71–75

[4] Monaghan J M and O'Reilly 1992 Machinability of aluminum alloy: Silicon carbide metal matrix composite. *Process Adv. Mater.* 2: 37–46

[5] Kalpakjian S, Steven R Schmid and Musa H 2013 *Manufacturing engineering and technology*. Sixth edition, Prentice Hall: London

[6] Pal S, Mitra R and Bhanuprasad V V 2008 Aging behaviour of Al–Cu–Mg alloy–SiC composites. *Mater. Sci. Eng. A* 480: 496–505

[7] Rajmohan T, Palanikumar K and Ranganathan S 2013 Evaluation of mechanical and wear properties of hybrid aluminium matrix composites. *Trans. Nonferrous Metallic Soc. China* 23: 2509–2517

[8] Shorowordi K M, Laoui T, Haseeb A S M A, Celis J P and Froyen L 2003 Microstructure and interface characteristics of

B_4C, SiC and Al_2O_3 reinforced Al matrix composites: A comparative study. *J. Mater. Process. Technol*. 142: 738–743

[9] Rajaram G, Kumaran S and Rao T S 2011 Influence of graphite and copper in mechanical properties of aluminum silicon alloy. *Trans. Indian Inst. Metals* 64(1–2): 53–56

[10] Senthilkumar N, Kalaichelvan K and Elangovan K 2012 Mechanical behavior of aluminum particulate epoxy composite-experimental study and numerical simulation. *Int. J. Mech. Mater. Eng*. 7(3): 214–221

[11] Pawade R S and Suhas S Joshi 2011 Multi-objective optimization of surface roughness and cutting forces in high-speed turning of Inconel 718 using Taguchi grey relational analysis (TGRA). *Int. J. Adv. Manuf. Technol.* 56: 47–62

[12] Senthilkumar N and Tamizharasan T 2014 Effect of tool geometry in turning AISI 1045 steel: Experimental investigation and FEM analysis. *Arabian J. Sci. Eng*. 39(6): 4963–4975

[13] Yang S H and Natarajan U 2009 Multi-objective optimization of cutting parameters in turning process using differential evolution and nondominated sorting genetic algorithm-II approaches. *Int. J. Adv. Manuf. Technol*. 49: 773–784

[14] Srinivas N and Deb K 1994 Multi-objective optimization using nondominated sorting in genetic algorithms. *Evolut. Comput*. 2(3): 221–248

[15] Palanikumar K, Latha B, Senthilkumar V S and Karthikeyan R 2009 Multiple performance optimization in machining of GFRP composites by a PCD tool using nondominated sorting genetic algorithm (NSGA-II). *Metals Mater. Int.* 15(2): 249–258

[16] Ranjith K Roy 2001 *Design of experiments using the Taguchi approach: 16 steps to product and process improvement*. Wiley-Interscience Publication: New York

[17] Raviraj Shetty, Raghuvir B Pai, Shrikanth S Rao and Rajesh Nayak 2009 Taguchi's technique in machining of metal matrix composites. *J. Brazilian Soc. Mech. Sci. Eng.* 31: 12–20

[18] Ross P J 1996 *Taguchi techniques for quality engineering: Loss function, orthogonal experiments, parameter, and tolerance design*. Second edition, McGraw-Hill, NewYork

[19] Senthilkumar N, Ganapathy T and Tamizharasan T 2014a Optimization of machining and geometrical parameters in turning process using Taguchi method. *Australian J. Mech. Eng*. 12(2): 233–246

[20] Ramanujam R, Muthukrishnan N and Raju R 2011 Optimization of cutting parameters for turning Al–SiC(10p) MMC using ANOVA and Grey relational analysis. *Int. J. Precision Eng. Manuf.* 12: 651–656

[21] Ranganathan S and Senthilvelan T 2011 Multi-response optimization of machining parameters in hot turning using Grey analysis. *Int. J. Adv. Manuf. Technol*. 56: 455–462

[22] Wang M Y and Lan T S 2008 Parametric optimization on multi-objective precision turning using Grey relational analysis. *Inform. Technol. J*. 7: 1072–1076

[23] Gopalsamy B M, Mondal B and Ghosh S 2009 Optimization of machining parameters for hard machining: Grey relational theory approach and ANOVA. *Int. J. Adv. Manuf. Technol*. 45: 1068–1086

[24] Suhail A H, Ismail N, Wong S V and Jalil N A A 2012 Surface roughness identification using the grey relational analysis with multiple performance characteristics in turning operations. *Arabian J. Sci. Eng*. 37(4): 1111–1117

[25] Tzeng C J, Lin Y H, Yang Y K and Jeng M C 2009 Optimization of turning operations with multiple performance characteristics using the Taguchi method and Grey relational analysis. *J. Mater. Process. Technol*. 209: 2753–2759

[26] Senthilkumar N, Tamizharasan T and Anandakrishnan V 2014b A Hybrid Taguchi–Grey relational technique and Cuckoo search algorithm for multi-criteria optimization in hard turning of AISI D3 steel. *J. Adv. Eng. Res*. 1(1): 16–31

[27] Gamst G, Meyers L S and Guarino A J 2008 *Analysis of variance designs – A conceptual and computational approach with SPSS and SAS*. Cambridge University Press: Cambridge, London

[28] Montgomery D C 2013 *Design and analysis of experiments*. Eight edition, Wiley, New York

[29] Chen J 2009 Multi-objective optimization of cutting parameters with improved NSGA-II. In: *Proceedings of International Conference on Management and Service Science, Wuhan*, 1–4

[30] Datta R and Deb K 2009 A classical-cum-evolutionary multi-objective optimization for optimal machining parameters. *World Congress on Nature and Biologically Inspired Computing*, Coimbatore, India, 607–612

[31] Datta R and Majumder A 2010 Optimization of turning process parameters using multi-objective evolutionary algorithm. *IEEE Congress on Evolutionary Computation*, Barcelona, Spain, 1–6

[32] Deb K and Datta R 2011 *Hybrid evolutionary multi-objective optimization of machining parameters*. KanGAL Report. 1–23

[33] Deb K, Pratap A, Agarwal S and Meyarivan T 2002 A fast and elitist multi-objective genetic algorithm: NSGA-II. *IEEE Trans. Evolut. Comput.* 6(2): 182–197

[34] Deb K and Goel T 2001 Controlled elitist nondominated sorting genetic algorithms for better convergence. *Evolutionary Multi-Criterion Optimization* 1993: 67–81

[35] Palanikumar K and Karthikeyan R 2006 Optimal machining conditions for turning of particulate metal matrix composites using Taguchi and response surface methodologies. *Mach. Sci. Technol*. 10(4): 417–433

[36] Senthilkumar N, Tamizharasan T and Gobikannan S 2014d Application of response surface methodology and firefly algorithm for optimizing multiple responses in turning AISI 1045 steel. *Arabian J. Sci. Eng.* 39(11): 8015–8030

[37] Hocheng H 2012 *Machining technology for composite materials: Principles and practice.* Woodhead Publishing Limited: UK

[38] Edward M Trent, Paul K Wright and Paul K Wright 2000 *Metal cutting*. Fourth edition, Butterworth–Heinemann: Woburn, MA

[39] Chadwick G and Froyen L 1991 *Metal matrix composites*, North Holland, New York, USA

[40] Brun M K and Lee M 1985 Wear characteristics of various hard materials for machining SiC-reinforced aluminum alloy. *Wear* 104: 21–29

[41] Senthilkumar N, Tamizharasan T and Anandakrishnan V 2014c Experimental investigation and performance analysis of cemented carbide inserts of different geometries using Taguchi-based Grey relational analysis. *Measurement* 58: 520–536

[42] Li J, Yang X, Ren C, Chen G and Wang Y 2015 Multi-objective optimization of cutting parameters in Ti–6Al–4V milling process using nondominated sorting genetic algorithm-II. *Int. J. Adv. Manuf. Technol*. 76(5): 941–953